Genij Ortopedii. 2021. Vol. 27, no. 6. P. 773-781.

Original article

https://doi.org/10.18019/1028-4427-2021-27-6-773-781

Development of porous titanium implants for interbody fusion

S.O. Ryabykh, T.A. Silant'eva, O. V. Dyuryagina, K.A. D'iachkov, M.V. Stogov✉, N.I. Antonov, N.V. Tushina, A.V. Reznik

Ilizarov National Medical Research Centre for Traumatology and Orthopedics, Kurgan, Russian Federation

Corresponding author: Maksim V. Stogov, stogo_off@list.ru

Abstract

Relevance Application of 3D printing using the method of selective laser fusion for production of intervertebral cages is a topical trend of the spinal surgery. **Purpose** Assessment of the efficiency and safety of original interbody fusion implant application made of titanium alloy according to 3D printing technology with selective laser fusion. **Materials and methods** The original flattened bean-shaped cages, with an integral side part and an internal configuration in the shape of three-dimensional 1.5 × 1.8 mm porous lattice were tested . The products were made of Ti6Al4V powder using 3D printing technology with selective laser fusion. Post-processing of the products surface included abrasive blast cleaning using the SLA method and sterilization with ethylene oxide. Experiments on modeling interbody fusion with replacement of intervertebral discs with cages at levels L4 – L5 and L5 – L6 were performed in 8 mongrels. Additional primary stabilization of the lumbar spine was produced with an external fixator within 30 days after implantation. The total follow-up period lasted 180 days. Radiography, scanning electron microscopy, roentgenospectral and biochemical analysis methods were applied. **Results** X-ray examination demonstrated the contact between the frontal surfaces of the cages and the bone tissue of the vertebral bodies and the development of fusion in all experimental animals. Biochemical analysis did not reveal the signs of intoxication, indicating the danger of the products application. The microrelief of the implants was characterized by microroughness ranged from 1to 50 μm. In the surface layer of products, in addition to the elements of titanium, aluminum and vanadium, the carbon, oxygen, silicon, trace amounts of other organic and inorganic elements were found. Newly formed bone trabeculae were macroscopically and submicroscopically visualized in the sawcuts of bone blocks in the porous lattice of the internal part of the implants. **Conclusions** Experimental testing of porous implants made of titanium alloy using selective laser fusion has shown their effectiveness in obtaining interbody fusion and acceptable safety.

Keywords: interbody fusion, implant, titanium alloy, selective laser fusion

For citation: Ryabykh S.O., Silant'eva T.A., Dyuryagina O.V., D'iachkov K.A.,Stogov M.V., Antonov N.I., Tushina N.V., Reznik A.V. Development of porous titanium implants for interbody fusion. *Genij Ortopedii*, 2021, vol. 27, no 6, pp. 773-781. https://doi.org/10.18019/1028-4427-2021-27-6-773-781.

Introduction of interbody fusion using implants made from biocompatible materials is a topical tendency in spine surgery. Porous implants made of titanium and its alloys are on the rise due to strong primary osteointegration with vertebral bodies, not requiring long additional fixation [1–4]. In metal powder industry the application of 3D-printing technology by selective laser melting opens up new opportunities in the fast and accessible production of medical devices [5, 6]. The advantages of this technology involve the application of 3D-modeling and the possibility of creating an adjustable macrostructure with improved mechanical characteristics for the production of standard or customized implants [6].

The purpose of the study is to evaluate the efficacy and safety of original interbody implant application for spinal fusion, made from a titanium alloy using selective laser fusion 3D-printing technology.

MATERIALS AND METHODS

Technical part Cages for the replacement of intervertebral discs of the lumbar spine [7] were produced using 3D-printing technology by selective laser melting (SLM) from Ti6Al4V powder with a cell size of < 100 μm, Rematitan CL brand (Dentaurum GmbH, Germany), approved for medical use [eight]. Thermal processing of the products was produced in an N41H muffle furnace (Nabertherm, Germany). The impactor was threaded on a workbench using hand tap.

The size and configuration of the implant were previously defined on the basis of CT data of the lumbar spine in 5 intact adult mongrels of both sexes weighing from 9 to 17 kg. The cage had a biconcave flat-bean shape (Fig. 1). The weight of the implant was 1.233 grams, the volume was 0.25 cm3, the frontal size was 12.8 mm (a 1), the dorso-ventral size was 8 mm (a 2) and the cranio-caudal size in the middle part was 4.8 mm (b 3) and in the lateral part 5.45 mm (b 4). The outer part of the implant (around the perimeter) was solid, the inner part had the form of a three-dimensional orthogonal lattice structure with cell sizes of 1.5 × 1.8 mm and bar diameters of 0.5–0.7 mm (a). Spikes of regular triangular shape were located in the central part of the anterior and posterior surfaces of the implant to increase the stability of bone fixation. The distance between the tops of the spikes was 7 mm. On the lateral surface of the implant, there was a platform for attaching the impactor, located at 30º angle to the vertical axis of the implant.

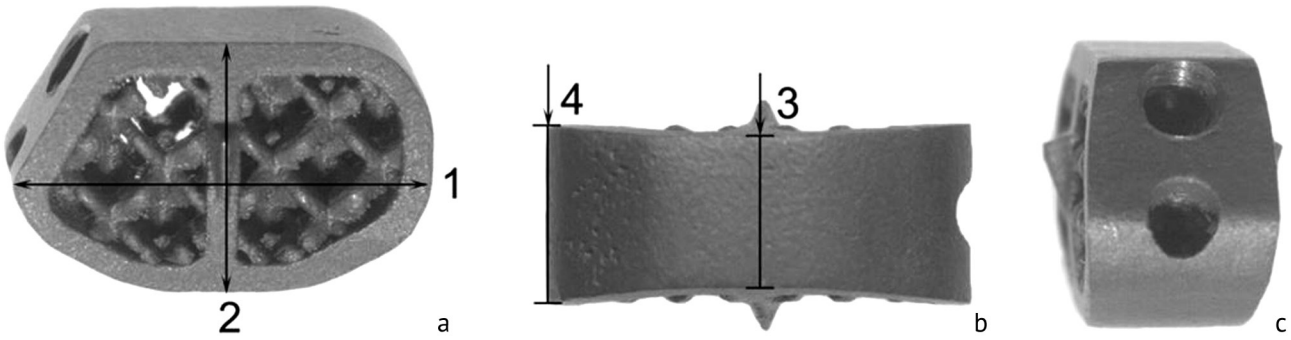

Fig. 1 View of original cage for interbody fusion: а – top view, б – front view, в – side view. Sizes of implant: 1 – front; 2 – dorso-ventral; 3, 4 – cranio-caudal

Post-processing of the products surface using SLA technique (Sand blasted, Largegrit, Acid-etched) included cleaning in Peenmatic 620 S sandblast machine (IEPCO, Switzerland) with abrasive Iepco Microblasting material MS90150 A of the following composition: SiC, SiO2, Al2O3, MgO and Na2O. The technology also provided for surface pickling with inorganic acids. That resulted in the following values of the roughness parameters - Ra 5–10 μm (arithmetic mean deviation of the profile) and Rz 25–50 μm (the highest profile height) were obtained. The products were sterilized with ethylene oxide in a Steri-Vac 5XL gas sterilizer (3M, USA).

Experimental part Cage implantation was performed in 8 mongrels of both sexes aged 1.5 to 3 years, weighing 9-17 kg. The minimal number of experimental animals was defined by the principles of humane experimental technique [9]. Surgical intervention involved discectomy performance and implants installation at L4-5 and L5-6, followed by stabilization of the lumbar spine with an external fixator modified by the authors [10]. On the 30th day after the operation, the device was disassembled. The follow-up was 180 days.

Clinical and laboratory examination of animals including evaluation of the general and local status was performed in order to assess the efficiency and safety of the product during the experiment. Radiography of the lumbar spine was performed in the dorsoventral and lateral views on 30^{th}, 90^{th}, and 180^{th} day to assess the process of osteointegration of the studied implants. The study was performed using Premium Vet X-ray device (Sedecal, Spain) with a Rotanode E7239 X-ray source (Toshiba, Japan). The current made up 3.2–2.5 mA, the voltage was 44.25–46.32 kV, the focal length was 97 cm and the exposure was set up automatically.

The maintenance and care of animals were regulated by SP 2.2.1.3218-14 "Sanitary and epidemiological requirements for the arrangement, equipment and management of experimental biological clinics (vivariums)"; GOST 33215-2014 “Guidelines for the housing and care of laboratory animals. Rules for equipping premises and organizing procedures”; GOST 33217-2014 “Guidelines for the housing and care of laboratory animals. Rules for the housing and care of laboratory mammal predators”. During the research, the requirements of the European Convention for the Protection of Vertebrate Animals used for experiments or for other scientific purposes and Directive 2010/63/EU of the European Parliament and the Council of the European Union for the protection of animals used for scientific purposes were observed.

Permission for the study was obtained from the Ethical Committee of the Federal State Budgetary Institution National Medical Research Center of Traumatology and Orthopaedics named after academician G.A. Ilizarov” (Protocol No. 2/57 dated May 17, 2018).

Electron microscopy examination of the implant surface The study of the chemical composition and microstructure of the implant surface (n = 4) was performed using the set of Zeiss EVO MA18 scanning microscope (Carl Zeiss Group, Germany) and BRUKER QUANTAX 200 - XFlash 6/10 energy dispersive spectrometer (Bruker Nano GmbH, Germany) at an accelerating voltage of 20 keV [11]. The sample was coated with thin current-conducting layer of about 10 nm thickness in an IB-6 ion sprayer (EICO, Japan). 5 typically located areas on the surface of each product were examined at hardware magnification ×3000. The surface microtopography was evaluated according to the following parameters: integrity, roughness, porosity and the size of individual particles. The method of energy-dispersive X-ray spectroscopy (EDS) was used to determine the local topographic distribution and the mass content of chemical elements (ω, %) in the surface layer of samples of 10 μm thickness. Data were collected, primarily processed and evaluated using ESPRIT software (Bruker Nano GmbH, Germany). The limitation was the sensitivity threshold of the EDC analysis of 0.02 weight percent.

Morphological study of bone blocks After sparing skeletization, the bone blocks, including adjacent vertebral bodies with implanted cage (n = 12), were sawn up in the sagittal plane and placed in paraform-glutaraldehyde fixator at 4 °C. Then the fragments were washed in phosphate buffer solution at pH 7.2, dehydrated in the series of ethanol

solutions with ascending concentration (from 70º to 100º), anhydrous acetone, and condensed in a mixture of epoxy resins for electron microscopy examination. The surface of epoxy blocks was polished with fine abrasive materials and coated with current-conducting layer in an IB-6 ion sprayer (EICO, Japan). Macrophotography of implants and polished surfaces of bone blocks was produced in a Stemi 2000-C stereo microscope using an AxioCam ERc5s digital camera and Zen blue software (Carl Zeiss MicroImaging GmbH, Germany). The study by scanning electron microscopy and EDS analysis was performed according to the above techniques.

Biochemical research The concentration of total protein, creatinine, C-reactive protein, oligopeptides, substances of low and average molecular weight (SLAMW) (including their catabolic pool) was defined in blood serum. The activity of the following enzymes was defined: alkaline and bone acid phosphatase (TRAP) and aminotransferase (ALT and AST). Definition of total protein, creatinine, C-reactive protein, and enzyme activity was produced in Hitachi 902 automatic biochemical analyzer (USA) using reagent kits from Vital Diagnostic (RF, St. Petersburg), BioSystem (Spain), and Vector Best (RF, Novosibirsk). The content of oligopeptides and SLAMW in blood serum was determined by the Malakhova method [12].

Statistical data analysis Statistical data processing of the RPR test was carried out using Microsoft Office Excel 2010 spreadsheet editor, including the AtteStat 13.1 add-in (I.P. Gaydyshev, Russia). The results were presented as sample means (M) and their standard deviations (SD). The results of the biochemical study were processed using the methods of nonparametric statistics. The significance of differences between the values obtained at the intervals of the experiment was compared with the values obtained before the operation (day 0). Intergroup differences were evaluated using the Wilcoxon test for dependent samples. Table data are presented as median, 25^{th}–75^{th} percentile.

RESULTS

Clinical observations In the first three days after the operation the general condition of the animals was moderate. Dogs mainly lay, there was a decrease in their support and motor function of the hind limbs. Feed and water intake was inactive. No disorder of the urinary system functions was observed. Body temperature ranged within 39–39.5º. In the area of surgical intervention, there was a moderate postoperative swelling of the soft tissues with moderate pain. There was no discharge from the surgical wound. Moderate serous discharge was observed from the sites of entry and exit of the wires.

From the third day after implantation, the signs of positive dynamics of postoperative course were observed. The behavior of the dogs got more active and the support and motor functions of the hind limbs were gradually restored. The appetite normalized. No dysfunction of the pelvic organs was observed. Body temperature had normal values of 38.5–39.0º. Tissue swelling in the area of the surgical wound decreased and no discharge from the suture was observed. Exudation from the entry and exit sites of the wires was insignificant. The removal of the external fixator on the 30th day after the operation did not cause aggravation of the general condition of the animals and reduction of the musculoskeletal function of the limbs.

Later, until the end of the study, the general condition of the animals was satisfactory, the dogs moved freely, and there were no disorders of the support function of the limbs (Fig. 2). The position of the hind limbs was correct. The axis of the spinal column remained visually straight during the entire observation period.

Radiographic studies On the day of surgery, the X-ray images show the location of implants in the interbody spaces of L4-5, L5-6 and their contact with the bone tissue of the vertebral bodies (Fig. 3, a, b).

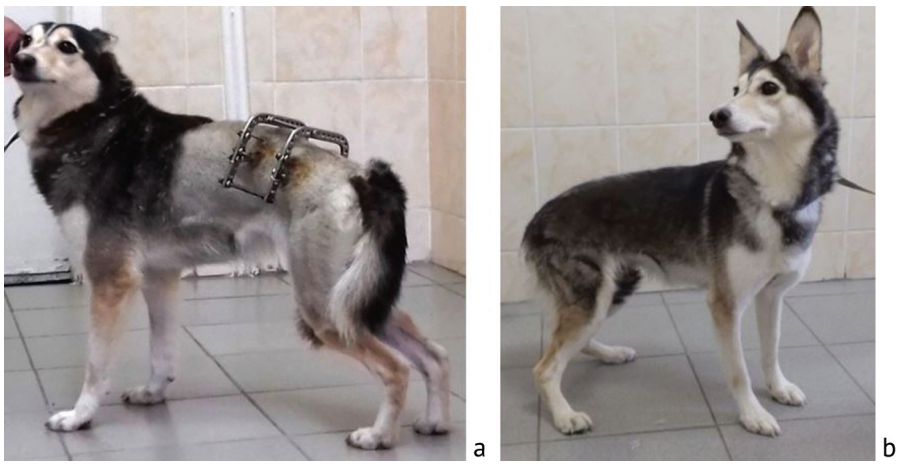

Fig. 2 Habitus of the experimental animal on 30^{th} (a) and 180^{th} (b) day of the experiment

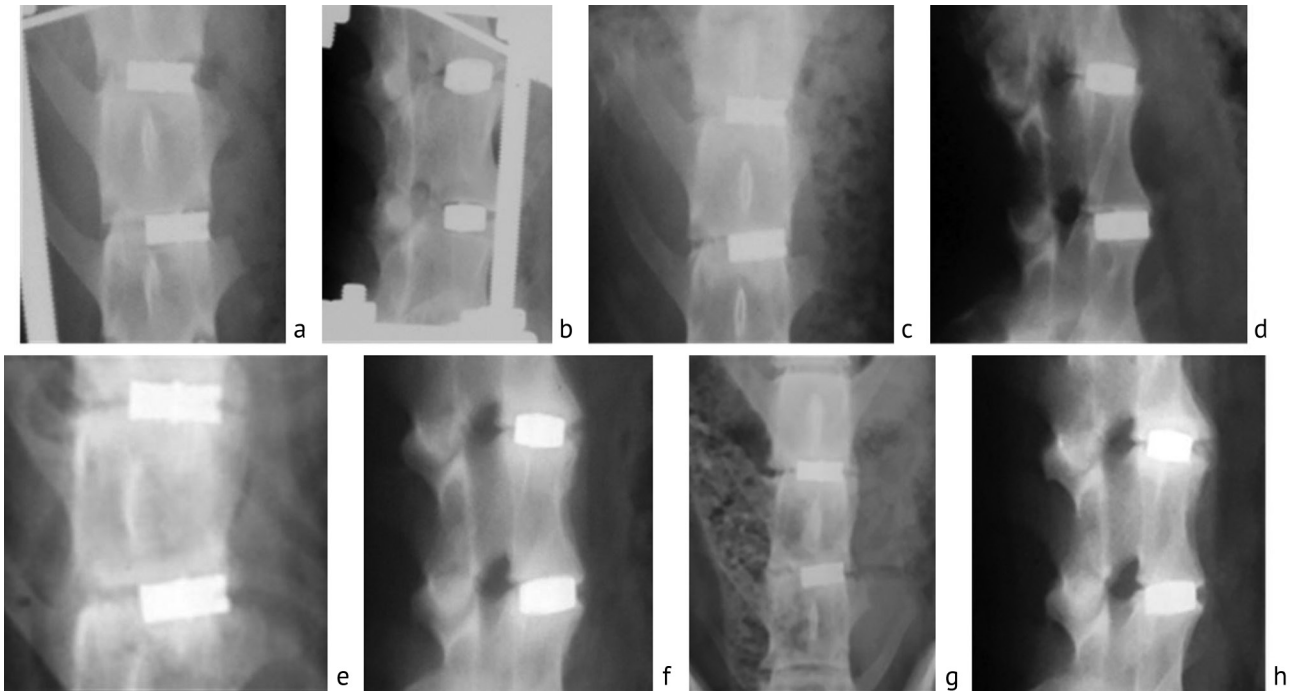

Fig. 3 The X-rays of the lumbar spine of the dog: on the day of surgery (a, b); in 30 (c, d), 90 (e, f) and 180 (g, h) days after the operation. In the left – AP view, in the right - lateral view

On the 30th day after the operation, the longitudinal axis of the spine was correct and no dislocation of the cages from the interdiscal spaces was observed. The line of the interbody space of the posterior portion of the intervertebral disc was clearly visible. The structure of the vertebral body was homogeneous, the line of the anterior contour of the vertebral bodies in the upper and lower sections looked irregular and slightly blurred. An increase of the radiological density of the host bone adjacent to the implants was observed. No decrease in radiological bone density along the perimeter of the cages was defined (Fig. 3, c, d).

In 90 days after operation, the longitudinal axis of the spine remained correct and no cage migration was observed. The structure of the vertebral body was homogeneous and the spread dense bone layers were observed in the anterior contour of the vertebral bodies in the upper and lower portions. Interbody spaces were poorly visible and were filled in with loose and intense shadows. The area of high radiological density of the bone tissue of the vertebrae adjacent to the implants was enlarged and took totally up to 1/3 of the volume of the vertebral bodies. Along the perimeter of the cages, a blurred thin lucent line of the same thickness was defined (Fig. 3, e, f).

On the 180th day after the operation, the longitudinal axis of the spine remained unchanged and no dislocation of the cages from the interdiscal spaces was observed. The shadow of the anterior contour of the vertebral bodies in the upper and lower parts became more distinct. Progression of the dorso-ventral size increase of the vertebral bodies was not observed. The density of the bone layers shadows were close to the same of the host bone tissue. The height of the interbody space decreased, but was clearly visible. The area of increased radiological density of the bone tissue of the vertebral bodies acquired limited contour. The lucent line around the cages was visible, but remained unchanged (Fig. 3, g, h).

The radiological pattern of the entire observation period showed favorable course of bone formation process in the "implant-bone" system such as an increase of bone density, increase of the dorso-ventral size of the vertebral bodies, the absence of cage dislocation and progression of bone resorption around the implants.

Scanning electron microscopy and energy dispersive radiological spectroscopy of the implant surface. Pronounced microroughness was defined in the studied areas of the samples. Developed surface relief comprised chaotically oriented extended protrusions and fissures of 1–20 μm; micropores with a diameter of less than 1 micron and polymorphic particles of 1–50 μm and less than 1 μm (Fig. 4a).

Composite (Fig. 4b) and individual EDS maps of the each sample surface showed uneven distribution of chemical elements. The titanium, vanadium, and aluminum metals predominating in the alloys were found over the entire analyzed area in the shape of overlapping spread accumulations. The highest content of silicon, carbon and aluminum elements was observed in the composition of morphologically identified particles. The distribution of oxygen and sodium was more regular with local concentration increase in particles with high content of aluminum and silicon.

Analysis of the EDS spectra made it possible to reveal the peculiarities of the composition and quantitative ratio of the chemical elements of the implants surface layer. Peaks of the characteristic radiation of titanium, aluminum, vanadium, carbon, oxygen, silicon, sodium, ferrum, nitrogen, magnesium, sulfur and chlorine were defined in the EDS spectrum (Fig. 4c).

Quantitative evaluation of the elemental chemical composition showed that the weight concentrations of chemical elements in the products surface layer differed significantly from their values in accordance with GOST R ISO 5832-3-2014 (Table 1).

The content of titanium and vanadium was reduced, and the concentrations of aluminum, oxygen, carbon, ferrum and nitrogen exceeded the standard indices. In addition, analytically defined amounts of silicon, traces of magnesium, chlorine and sulfur were present.

Morphological study of bone blocks Ingrowth of the newly formed bone substance into the pores of the implants was observed in macropreparations and electronic scans of operated vertebral bodies sawcuts (Fig. 5).

At the same time, the thickness of the fibrous capsule around the structural elements of the implant ranged within 0.1–5 mm, and the cage was fixed in the bone by forming a network of bone trabeculae in the internal space of the lattice, mainly without contact with metal surfaces (Fig. 5b). Composite EDS maps show the mutual arrangement of calcium bone trabeculae, carbon fibrous components of the fibrous sheath and titanium structural elements of cages, demonstrating the mechanisms of intraosseous fixation of the cage (Fig. 5c).

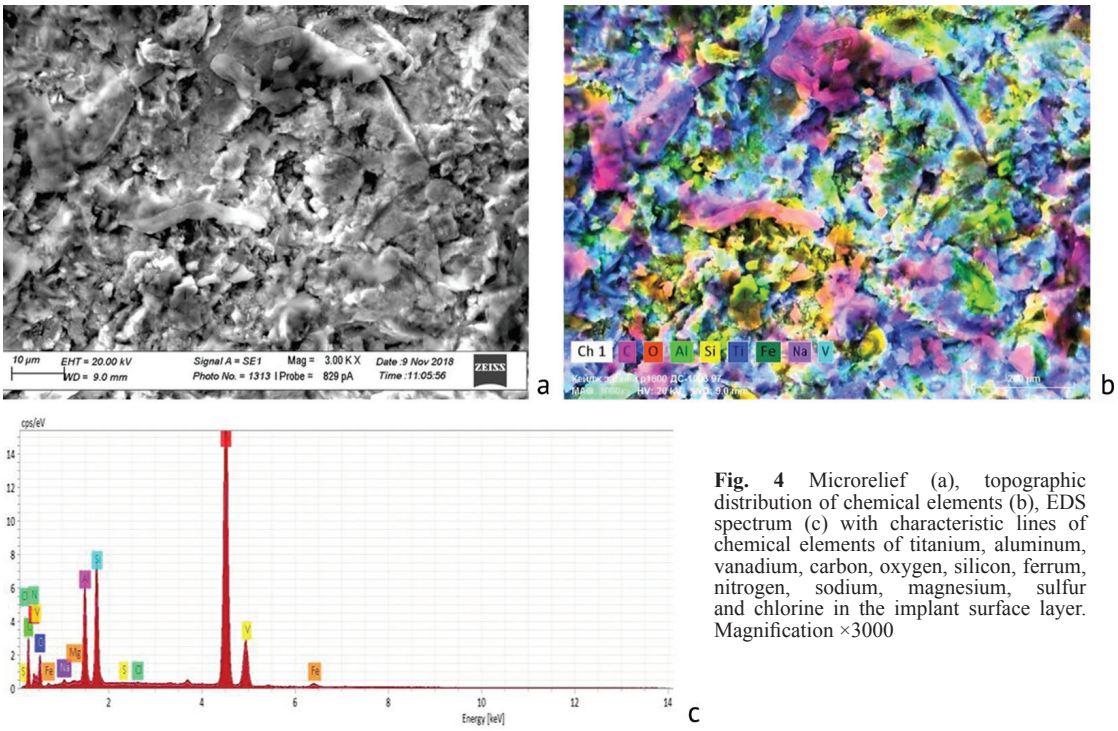

Fig. 4 Microrelief (a), topographic distribution of chemical elements (b), EDS spectrum (c) with characteristic lines of chemical elements of titanium, aluminum, vanadium, carbon, oxygen, silicon, ferrum, nitrogen, sodium, magnesium, sulfur and chlorine in the implant surface layer. Magnification ×3000

Table 1

Elemental chemical composition of materials in implant surface layer (ω, %)

Element	GOST R ISO 5832-3-2014	Implant surface	
		M	SD
Titanium	≥ 88	46.6	3.71
Aluminum	5.5–6.75	7.6	0.50
Vanadium	3.5–4.5	1.3	0.15
Oxygen	0.2	16.7	0.73
Carbon	≤ 0.08	19.0	3.32
Silicon	–	6.9	0.47
Sodium	–	0.6	0.05
Ferrum	≤ 0.3	0.8	0.27
Nitrogen	≤ 0.05	0.3	0.21
Magnesium	–	0.2	0.04
chlorine	–	0.1	0.04
Sulfur	–	0.05	0.021

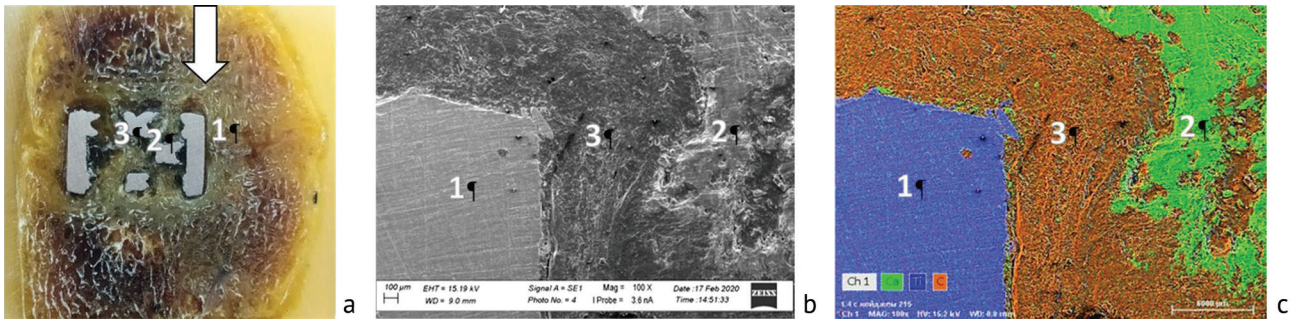

Fig. 5 Intraosseous integration of the implant in the L4-L5 interbody space in 180 days after anterior fusion modeling. Intergrowth of a newly formed bone into the pores of large-mesh implant without contact with metal surfaces: 1 – implant; 2 – bone tissue; 3 – fibrous tissue. The arrow in the image of the bone block sawcut (a) indicates the location of the scanning area (b) and EDS mapping (c). Compositional EDS map (b) was obtained in the characteristic radiation of titanium (blue), calcium (green) and carbon (orange); b, c – magnif.100

The results of biochemical study showed that the activity of alkaline phosphatase in the blood serum of dogs at certain periods of the experiment was statistically significantly high and the activity of the bone acid phosphatase isoenzyme was lower than the initial values (Table 2). Significant deviations of the levels of total protein, creatinine, aminotransferases (not given in the Table) with regards to preoperative values were not found. No increase in the total content of endogenous intoxication products (the level of SLAMW and their catabolic pool) in the blood of dogs was observed. On the 30th day after implantation statistically significant increase of the level of C-reactive protein in the blood serum of experimental animals was stated.

In general, it can be stated that the signs of more intensive bone formation were observed in animals (increase of alkaline phosphatase level with TRAP decrease) on the 30-60th day of implantation. No toxic manifestations indicating the unacceptable safety of the studied products application were found in experimental animals.

Table 2

Dynamics of biochemical indices changes in blood serum of dogs at different stages of the experiment (Median, 25th–75th percentile)

Index	Day after operation						
	0	30	60	90	182	270	365
Alkaline phosphatase, U/l	48 (38–68)	74* (69–117)	77* (66–102)	54 (45–90)	46 (39–78)	52 (48–54)	66 (53–90)
Acid phosphatase, U/l	5.5 (4.6–7.1)	3.2* (2.8–3.6)	4.2* (3.6–4.7)	3.8* (3.3–4.3)	5.9 (4.6–6.6)	6.7 (5.9–7.1)	6.0 (5.7–6.2)
Total protein, g/l	64 (61–66)	69 (65–71)	66 (63–68)	65 (63–68)	63 (60–67)	63 (61–68)	66 (65–67)
Creatinine, µmol/l	83 (77–88)	64 (61–73)	73 (64–80)	81 (76–84)	89 (81–97)	75 (73–81)	90 (89–91)
C-reactive protein, mg/l	0,0	5.9* (2.0–8.5)	0.0 (0.0–0.6)	0,0	0,0	0,0	0.0 (0.0–5.4)
SLAMW, opt.den.unit	5.9 (5.6–6.8)	5.9 (5.6–6.6)	5.5 (4.6–6.6)	5.8 (5.1–7.1)	6.3 (4.9–6.8)	5.1 (4.7–6.0)	6.1 (5.9–6.2)
Cat.pool SLAMW, %	19 (13–20)	18 (16–21)	16 (10–19)	18 (15–20)	16 (13–19)	16 (10–19)	14 (13–17)

Note: * – significant differences with preoperative indices in $p < 0,05$.

DISCUSSION

Active introduction of precision 3D-printing technologies for production of the metal implants is caused by the need to fill in the bone defects of complex shape when autologous bone material is not available [13]. This solution is especially topical for surgical correction and stabilization of the spinal segments [1].

Multiple studies indicated that successful osteointegration of implants required the observance of several basic principles, i.e. strong primary fixation, application of biocompatible material and the porous and rough product surface [13, 14].

We met the requirement of primary stabilization of the lumbar spine in the area of cage placement using additional external fixation with the device that had previously proven its efficiency [15]. Radiologically confirmed absence of dislocation of the implants and

progressive resorption of the surrounding bone tissue witnessed the success of the chosen surgical tactics.

Bioinert titanium and its alloys are successfully used in traumatology and orthopedics, including the creation of various types of porous cages for interbody fusion [1, 2, 16]. Orthopedic metal implants directly contact the bone tissue, therefore, they need to have surface properties that ensure their osteointegration [1, 16]. It was stated that pore size of at least 100–200 μm provides fixation of products due to the bone ingrowth to a depth of 2–3 mm [13], and the optimal roughness values range from 1–2 and to more than 2 μm [14]. Experiments in sheep and rats demonstrated successful osteointegration of cylindrical porous implants made of Ti6Al4V alloy using the SLM technology and implanted into the femoral and tibial metaphyses [17–19]. Palmquist et al. performed surface sandblasting with the powder material of the implant without specifying the achieved roughness values and after that the products were cleansed with ultrasound [19]. Obaton et al. and Ran et al. did not apply finishing but used ultrasonic cleansing of the product surface [17, 18]. Bone tissue was found in pores in 2 months [17] and in 6 months after implantation [19]. In comparing the results with dependance on the pore sizes of 500, 600, 700, 900, and 1200 μm, the largest amount of bone tissue was found in lattice structure with pore diameter of 600 and 900 μm [17, 18].

In our experimental study, the vertebral bodies were stabilized with the external fixator for up to 30 days after implantation and after that the strength of the achieved fusion was defined by the intraosseous integration of the implants. At the end of the experiment, porous bone substance was found in the pores of implants with an average size of 1.5–1.8 mm. The mean surface roughness was 5–10 μm, i.e. being optimal for cage osteointegration.

However, morphological observations did not confirm osteoconduction since tight contact between the product surface and the newly formed bone tissue, that ensures its full osteointegration [20]. It should be noted that, unlike the above experimental models [17–19], the model of interbody fusion that we used provided cyclic biomechanical weightbearing on the implant. The mobility of the bodies of adjacent vertebrae in the area of implantation was revealed to the greatest extent after the removal of the external fixator. Probably, the micromotion of the vertebral bodies could activate the remodeling of the bone tissue and the formation of fibrous capsule around the implant.

In addition, the peculiarities of tissue integration of products depend on the chemical composition of their surface [13, 14, 16, 21–23]. It is known that the biocompatibility of titanium implants is provided by superficial fixation of serum and morphogenetic proteins and free calcium on negatively charged TiO oxide film being a favorable factor for osteoblast adhesion and subsequent stages of osteogenesis [14, 21]. Anyway, the implants processing using the common SLA technology allowing to create an optimal roughness of 2–5 microns leads to the impregnation of their surface by the particles of the implant itself and the abrasive and fatigue macro- and micro-fissure [22, 23]. Evaluation of the reasons for unsuccessful placement of titanium implants showed that in 96% of cases the surface layer of the products contains large amount of impurity particles of aluminum oxide and other chemical elements. Superficial contamination results in infection, pain and, finally, aseptic loosening and destruction of the implant [23, 24].

It was stated that microparticles of titanium and its alloys, even at low concentrations, stimulated the proliferation of fibroblasts, that contributes to the development of fibrous capsule and reduction of the stability of implant fixation [23]. Aluminum in Ti-Al-V systems increases the strength properties, and vanadium improves the ductility of the alloys [25]. However, vanadium and aluminum ions diffusely migrating from microparticles significantly reduce the mineralization of bone tissue and also inhibit erythropoiesis [26, 27]. Regardless the fact that Al2O3 is biocompatible and is used in medicine for the production of implants, including spine surgery [1, 28], its microparticles are the foreign bodies and the sources of cytotoxic ions diffusion. Silicon bioactive materials are also used for the production of implants in traumatology and orthopedics [16], however, concentration-dependent cytotoxicity of SiO2 particles has been proven [29].

Contamination of the implant surface with microparticles containing, in addition to the alloy components, silicon and trace amounts of other elements, could also be the cause of the fibrous capsule formation. Nevertheless, the relatively large pore size, 1500–1800 μm, probably, contributed to the reduction of the fibrogenic effect in the central part of the pores. Therefore, the ingrowth of the newly formed bone tissue without close contact with metal surfaces was observed. However, evaluation of the clinical observation results and laboratory studies did not reveal the signs of the implanted devices toxicity. In the future, we plan to additionally cleanse the cages using ultrasonic methods.

The experimental study indicated the efficiency and safety of porous cages application for interbody fusion made of titanium alloy using 3D-printing technology by selective laser melting. Elaborated design in combination with surface microstructuring technologies, allowed us to provide strong primary fusion resulting from active osteogenesis inside the porous structures of the implants. The results indicate the acceptable safety of the developed products application.

Small sample size should be considered limitation of the study, however, the number of experimental

animals was sufficient to obtain homogeneous results. In addition, the late implantation follow-up of the remodeling process of newly formed bone tissue in the pores products has not been studied.

CONCLUSIONS

The application of porous implants of an original design for interbody fusion, fabricated from Ti6Al4V powder using selective laser fusion technology, in combination with temporary extrafocal fixation of the spine is effective and safe. Primary fusion is formed within a month and persists throughout the entire postoperative period. The pore size of 1500–1800 μm provides the ingrowth of trabeculae of the newly formed bone substance throughout the entire volume of the implant.

REFERENCES

1. Babkin A.V. Implantaty pozvonkov dlia mezhtelovogo spondilodeza: biomekhanicheskie i tekhnicheskie idei, klinicheskie aspekty [Vertebral implants for interbody spondylodesis: biomechanical and technical ideas, clinical aspects]. *Voennaia Meditsina*, 2018, no. 4 (49), pp. 66-77. (in Russian)
2. Nuraliyev Kh.A. Zadnii mezhtelovoi spondilodez s ispolzovaniem keidzha v sisteme lecheniia osteokhondroza poiasnichnogo otdela pozvonochnika [Posterior interbody spondylodesis using a cage in the system of lumbar osteochondrosis treatment]. *Genij Ortopedii*, 2010, no. 4, pp. 68-72. (in Russian)
3. Naumov D.G., Mushkin A.Iu., Pershin A.A. Sovremennye vozmozhnosti khirurgicheskogo lecheniia infektsionnykh spondilitov u detei [Current possibilities of surgical treatment for infectious spondylitis in children]. *Genij Ortopedii*, 2017, vol. 23, no. 2, pp. 162-167.
4. Mukhametov U.F., Liulin S.V., Meshcheriagina I.A. Izuchenie otdalennykh rezultatov perednego spondilodeza s primeneniem razlichnykh vidov plastiki defekta pri khirurgicheskom lechenii povrezhdenii i zabolevanii pozvonochnika (obzor literatury) [Review of long-term results of anterior spondylodesis with different plasty applied for surgical treatment of spine injuries and diseases (literature review)]. *Genij Ortopedii*, 2017, vol. 23, no. 2, pp. 236-240.
5. Gubin A.V., Kuznetsov V.P., Borzunov D.Y., Koriukov A.A., Reznik A.V., Chevardin A.Iu. Problemy i perspektivy primeneniia additivnykh tekhnologii pri izgotovlenii kastomizirovannykh implantatov dlia travmatologii i ortopedii [Problems and prospects of using additive technologies in the manufacture of customized implants for traumatology and orthopedics]. *Meditsinskaia Tekhnika*, 2016, no. 4 (298), pp. 52-55. (in Russian)
6. Kilina P.N., Morozov E.A., Khanov A.M. Sozdanie implantatov s iacheistoi strukturoi metodom selektivnogo lazernogo spekaniia [Creation of implants with a meshy structure by selective laser sintering]. Izvestiia Samarskogo Nauchnogo Tsentra Rossiiskoi Akademii Nauk, 2015, vol. 17, no. 2-4, pp. 779-781. (in Russian)
7. Mikhailov D.A., Ptashnikov D.A. *Implantat dlia perednego spondilodeza pozvonochnika v poiasnichnom otdele* [The implant for anterior spinal spondylodesis in the lumbar spine]. Patent RF no. 176259, A 61 F 2/44, 2017. (in Russian)
8. *GOST R ISO 5832-3-2014. Implantaty dlia khirurgii. Metallicheskie materialy. Chast 3. Deformiruemyi splav na osnove titana, 6-aliuminiia i 4-vanadiia* [State Standard 5832-3-2014. Implants for surgery. Metallic materials. Part 3. Deformable alloy based on titanium, 6-aluminum and 4-vanadium]. M., Standartinform Publ., 2015, 5 p. (in Russian)
9. Russell W.M.S., Burch R.L. *The Principles of Humane Experimental Technique*. London, Methuen & Co, 1959, 252 p. DOI: 10.5694/j.1326-5377.1960.tb73127.x.
10. Kirsanov K.P., Menshchikova I.A., Diuriagina O.V., Timofeev V.N. *Apparat dlia lecheniia povrezhdenii i zabolevanii sheinogo otdela pozvonochnika zhivotnykh* [The device for the treatment of injuries and diseases of the cervical spine of animals]. Author's license no. 28819, A 61 D 1/00, 2002. (in Russian)
11. *GOST R ISO 22309-2015. Mikroanaliz elektronno-zondovyi. Kolichestvennyi analiz s ispolzovaniem energodispersionnoi spektrometrii dlia elementov s atomnym nomerom ot 11 (Na) i vyshe* [State Standard 22309-2015. Electron probe microanalysis. Quantitative analysis using energy dispersive spectrometry for elements with atomic numbers 11 (Na) and above]. M., Standartinform Publ., 2019, 24 p. (in Russian)
12. Danilova L.A., Basharina O.B., Krasnikova E.N., Litvinenko L.A., Ramenskaia N.P., Fomenko M.O., Mashek O.N.; Danilova L.A., editor. *Spravochnik po laboratornym metodam issledovaniia* [Laboratory Research Methods Handbook]. SPb., Piter, 2003, 733 p. (in Russian)
13. Tikhilov R.M., Shubniakov I.I., Denisov A.O., Konev V.A., Gofman I.V., Mikhailova P.M., Netylko G.I., Vasilev A.V., Anisimova L.O., Bilyk S.S. Kostnaia i miagkotkannaia integratsiia poristykh titanovykh implantatov (eksperimentalnoe issledovanie) [Bone and soft tissue integration of porous titanium implants (an experimental study)]. *Travmatologiia i Ortopediia Rossii*, 2018, vol. 24, no. 2, pp. 95-107. (in Russian) DOI: 10.21823/2311-2905-2018-24-2-95-107.
14. Vishnevskii A.A., Kazbanov V.V., Batalov M.S. Perspektivy primeneniia titanovykh implantatov s zadannymi osteogennymi svoistvami [Prospects for the use of titanium implants with prescribed osteogenic properties]. *Khirurgiia Pozvonochnika*, 2016, vol. 13, no. 1, pp. 50-58. (in Russian) DOI: 10.14531/ss2016.1.50-58.
15. Berdiugin K.A., Berdiugina O.V. Osteosintez pozvonochnika apparatami vneshnei fiksatsii [Osteosynthesis of the spine with external fixation devices]. *Fundamentalnye Issledovaniia*, 2013, no. 9 (part 4), pp. 765-768. (in Russian)
16. Popkov A.V. Biosovmestimye implantaty v travmatologii i ortopedii (obzor literatury) [Biocompatible implants in traumatology and orthopedics]. *Genij Ortopedii*, 2014, no. 3, pp. 94-99. (in Russian)
17. Obaton A.F., Fain J., Djemaï M., Meinel D., Léonard F., Mahé E., Lécuelle B., Fouchet J.J., Bruno G. In vivo XCT bone characterization of lattice structured implants fabricated by additive manufacturing. *Heliyon*, 2017, vol. 3, no. 8, pp. e00374. DOI: 10.1016/j.heliyon.2017.e00374.
18. Ran Q., Yang W., Hu Y., Shen X., Yu Y., Xiang Y., Cai K. Osteogenesis of 3D printed porous Ti6Al4V implants with different pore sizes. *J. Mech. Behav. Biomed. Mater*., 2018, vol. 84, pp. 1-11. DOI:10.1016/j.jmbbm.2018.04.010.
19. Palmquist A., Shah F.A., Emanuelsson L., Omar O., Suska F. A technique for evaluating bone ingrowth into 3D printed, porous Ti6Al4V implants accurately using X-ray micro-computed tomography and histomorphometry. *Micron*, 2017, vol. 94, pp. 1-8. DOI:10.1016/j.micron.2016.11.009.
20. Talashova I.A., Silant'eva T.A., Kononovich N.A., Luneva S.N. Biosovmestimost kaltsiifosfatnykh materialov biogennogo proiskhozhdeniia pri implantatsii v oblast defektov kostei sobak [Biogenic calcium phosphate materials implanted into canine bone defects and their biocompatibility]. *Genij Ortopedii*, 2016, no. 4, pp. 95-103. (in Russian)
21. Savich V.V., Saroka D.I., Kiselev M.G., Makarenko M.V. *Modifikatsiia poverkhnosti titanovykh implantatov i ee vliianie na ikh fiziko-khimicheskie i biomekhanicheskie parametry v biologicheskikh sredakh: monografiia* [Modification of the surface of titanium implants and its influence on their physicochemical and biomechanical parameters in biological media: monograph]. Minsk, Belarusskaia nauka, 2012, 244 p. (in Russian)
22. Vinnikov L.I., Savranskii F.Z., Simakhov R.V., Grishin P.O. Sravnitelnaia otsenka poverkhnostei implantatov, obrabotannykh tekhnologiiami SLA, RBM i Clean & PorousTM [Comparative evaluation of implant surfaces treated with SLA, RBM and Clean & PorousTM technologies]. *Dentalnaia Implantologiia i Khirurgiia*, 2016, no. 1 (22), pp. 52-56. (in Russian)
23. Rozhnova O.M., Pavlov V.V., Sadovoi M.A. Biologicheskaia sovmestimost meditsinskikh izdelii na osnove metallov, prichiny formirovaniia patologicheskoi reaktivnosti (obzor inostrannoi literatury) [Biological compatibility of medical devices based on metals, the reasons for the formation of pathological reactivity (review of foreign literature)]. *Biulleten Sibirskoi Meditsiny*, 2015, vol. 14, no. 4, pp. 110-118. (in Russian)

24. Tinkov V.A., Gorobets E.V., Likhota A.N., Rozova E.V., Makeeva I.N., Iatsenko L.F. Issledovanie poverkhnosti dentalnykh titanovykh implantatov metodom rastrovoi elektronnoi mikroskopii [Study of the surface of dental titanium implants by scanning electron microscopy]. *Metallofizika i Noveishie Tekhnologii*, 2012, vol. 34, no. 7, pp. 919-933. (in Russian)
25. Egorov A.A., Drovosekov M.N., Aronov A.M., Rozhnova O.M., Egorova O.P. Sravnitelnaia kharakteristika materialov, primeniaemykh v stomatologicheskoi implantatsii [Comparative characteristics of materials used in dental implantation]. *Biulleten Sibirskoi Meditsiny*, 2014, vol. 13, no. 6, pp. 41-47. (in Russian) DOI: 10.20538/1682-0363-2014-6-41-47.
26. Chertov S.A., Stoikov S.V. Obzor svoistv materialov, ispolzuemykh v proizvodstve dentalnykh implantatov [Overview of the properties of materials used in the manufacture of dental implants]. *Ukraïnskii Stomatologichnii Almanakh*, 2013, no. 4, pp. 101-104. (in Russian) Available at: http://nbuv.gov.ua/UJRN/Usa_2013_4_29.
27. Vorobeva N.M., Fedorova E.V., Baranova N.I. Vanadii: biologicheskaia rol, toksikologiia i farmakologicheskoe primenenie [Vanadium: biological role, toxicology and pharmacological application]. *Biosfera*, 2013, vol. 5, no. 1, pp. 077-096. (in Russian)
28. Abyzov A.M. Oksid aliuminiia i aliumooksidnaia keramika (obzor). Chast 1. Svoistva Al2O3 i promyshlennoe proizvodstvo dispersnogo Al2O3 [Aluminum oxide and alumina ceramics (Review). Part 1. Properties of Al2O3 and industrial production of dispersed Al2O3]. *Novye Ogneupory*, 2019, no. 1, pp. 16-23. (in Russian) DOI: 10.17073/1683-4518-2019-1-16-23.
29. Andreev G.B., Minashkin V.M., Nevskii I.A., Putilov A.V. Materialy, proizvodimye po nanotekhnologiiam: potentsialnyi risk pri poluchenii i ispolzovanii [Materials produced by nanotechnology: potential risks during production and use]. *Rosciiskii Khimicheskii Zhurnal*, 2008, vol. 52, no. 5, pp. 32-38. (in Russian)

The article was submitted 11.11.2020; approved after reviewing 25.01.2021; accepted for publication 19.10.2021.

ИInformation about the authors:

1. Sergey O. Ryabykh – Doctor of Medical Sciences, rso_@mail.ru;
2. Tamara A. Silant'eva – Candidate of Biological Sciences, tsyl@mail.ru;
3. Olga V. Dyuryagina – Candidate of Veterinary Sciences, diuriagina@mail.ru;
4. Konstantin A. D'iachkov – Doctor of Medical Sciences, dka_doc@mail.ru;
5. Maksim V. Stogov – Doctor of Medical Sciences, stogo_off@list.ru;
6. Nikolay I. Antonov – Candidate of Biological Sciences;
7. Natalia V. Tushina.
8. Artem V. Reznik – M.D.

Financing *The article was prepared within the framework of the topic "Development and evaluation of the efficiency the patient-oriented implants application in axial skeleton surgery" according to the Government Statement for the implementation of scientific research and development of the Federal State Budgetary Institution "National Medical Research Center for Traumatology and Orthopedics named after Academician G.A. Ilizarov", Ministry of Health of Russia".*